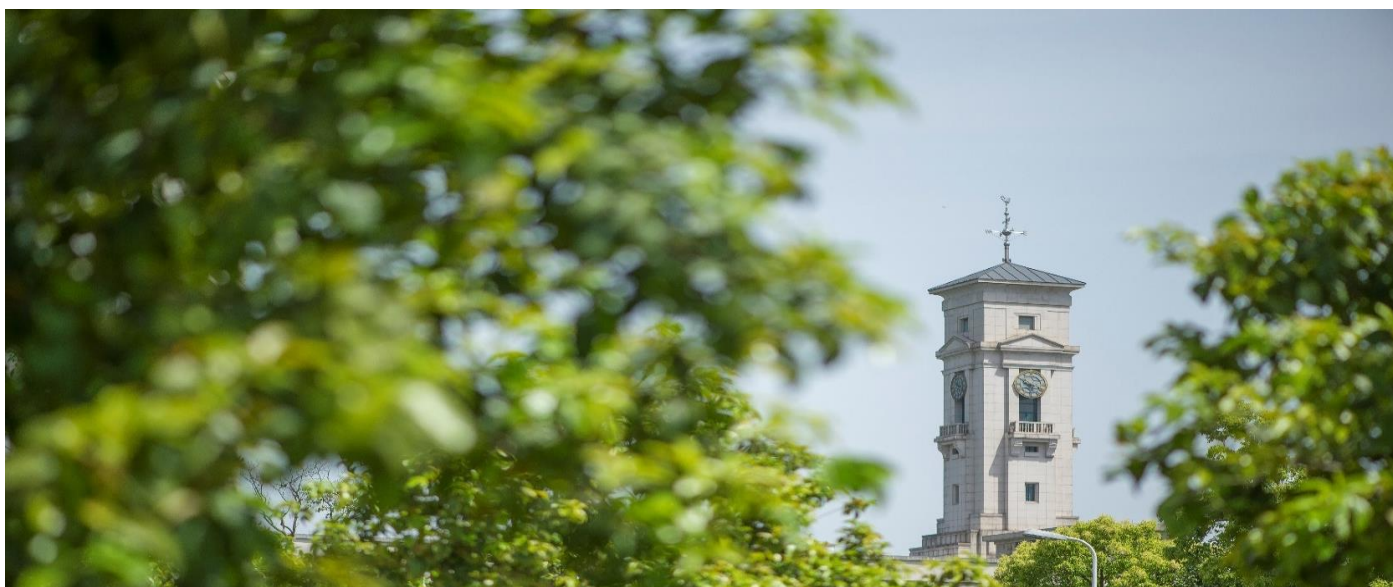# Magnetically-accelerated photo-thermal conversion and energy storage based on bionic porous nanoparticles

Lei Shi, Yanwei Hu, Daili Feng, Yurong He, Yuying Yan,

University of Nottingham
UK | CHINA | MALAYSIA

University of Nottingham Ningbo China, 199 Taikang East Road, Ningbo, 315100, Zhejiang, China.

First published 2020

University of
Nottingham
UK | CHINA | MALAYSIA

Magnetically-accelerated photo-thermal conversion and energy storage based on bionic porous nanoparticles

Lei Shi[a,b,c], Yanwei Hu[a,b], Daili Feng[c], Yurong He[a,b]*, Yuying Yan[c,d]

a School of Energy Science and Engineering, Harbin Institute of Technology, Harbin 150001 China

b Heilongjiang Key Laboratory of New Energy Storage Materials and Processes, Harbin 150001 China

c Fluids & Thermal Engineering Research Group, Faculty of Engineering, University of Nottingham, NG7 2RD, UK

d Research Centre for Fluids and Thermal Engineering, University of Nottingham Ningbo China, Ningbo 315100, China

*Corresponding author. E-mail address: rong@hit.edu.cn

Abstract: Recently, the technology of mixing phase change materials with high thermal conductivity fillers was developed, which has allowed thermal energy storage to be implemented in a wide range of industrial technologies and processes. In the present study, a hierarchical bionic porous nano-composite was prepared, which efficiently merged the nanomaterial characteristics of magnetism and high thermal conductivity in order to form a magnetically-accelerated solar-thermal energy storage method. The morphology and thermo-physical properties of materials were analysed. The experimental outcomes of phase change heat transfer demonstrated that the maximum storage efficiency increases by 102.7% when the hierarchical bionic porous structure is used, and a further 27.1% improvement can be achieved with the magnetic field. At the same time, the heat transfer process of energy storage in hierarchical porous composites under external physical fields is explained by simulation. Therefore, this magnetically-accelerated method demonstrated the superior solar-thermal energy storage characteristics within a hierarchical bionic porous structure which is particularly beneficial for the utilisation of solar direct absorption collectors and energy storage technology.

Keywords: Phase change material; nanoparticles; photo-thermal conversion; magnetic field

1. Introduction

The world's energy consumption has increased, due to the drastic development of human society which has caused global warming and environmental pollution [1,2]. As an excellent renewable energy source which can substitute fossil fuels, solar energy has successfully gained attention due to its environmental friendliness and lower cost [3-6]. Solar-thermal conversion depends on direct absorption solar collectors and has become a good method for harnessing solar energy [7-10]. In addition, it is the main cause of spreading industrial applications, such as thermal energy storage and

electricity and steam generation [11]. Solar-thermal energy storage is considered to be a key feature in sustainable solar-thermal conversion requests [12]. Through improvement in heat storage capacity and solar absorption ability, this is important for widely applying solar-thermal energy storage [13]. Therefore, thermal energy storage structures and materials are two important aspects which are often explored by researchers.

When it comes to energy storage structures, pore-based shape-stabilised composite is more obtainable and profitable for exploring other excellent properties such as thermal conduction and flame retardancy comparing with a single organic or inorganic material, eutectics and mixtures and encapsulated phase change materials (PCMs) [14,15]. Currently, the hierarchical porous material is considered as a developing type of porous material which possesses a variety of levels of structure and porosity [16]. This helps in presenting the unique scale benefits from micro pores to a macro level [17]. Due to their integrated hierarchical porosity with a variety of length scales, they are quite suitable for mass loading and diffusion, electron and ion transport, and light-harvesting, because they are used for converting solar and chemical energy on a wider level [18,19]. The hierarchical porous architecture causes degradation to the structure of energy shortage and fast heat transfer incurred by volume expansion during the charge cycle process [20]. This process is also important for light-harvesting via multiple light reflections and scattering [21]. However, the machines of effect of hierarchically porous materials on their functions are not only simple micro-scale structures, but they also include structural parameters at different scales and interactions with each other [22]. The theory of flow and heat transfer in hierarchically porous materials has not been reported systematically, and there are still great challenges which must be faced in the development of hierarchically porous materials for thermal energy storage [23].

Furthermore, thermal energy storage is achieved due to a change in internal energy material, such as chemical energy, latent heat, and sensible heat [24,25]. From the existing thermal energy shortage methods, latent heat storage is considered as a reliable and efficient method due to the solid-liquid phase material change [26-29], mostly due to the fact that it has a high density of thermal storage in a small volume change as well as a small temperature region during thermal energy storage [30, 31]. Phase change materials have the ability to absorb latent heat at the time of transition into liquid from a solid which is appropriate for storing solar-thermal energy [32,33]. In liquid PCMs, when nanoparticles are added, this results in nanofluid PCMs which possess high storage capacity and heat transfer, compared to one-component PCMs, such as paraffin wax and hydrated salts [34-36]. For example, a research experiment was conducted in order to determine the effects of nickel nanoparticle mass concentration on the performance of phase change in PCMs by Oya et al. [37]. The percolation clusters caused a high upsurge in determined heat conduction. Nourani et al. [38] created an original

paraffin/Al_2O_3 mixture which exhibited enhanced thermal conductivity and reliability. However, very little research has been conducted on solar-thermal PCM systems on the basis of nanofluid PCMs, allowing separate expansion of the conversion of solar-thermal efficiency after applying the external physical fields, such as magnetic, sound, electric field [39-41], let alone studying the heat transfer process of solar-thermal storage and energy conversion in hierarchically porous structures under external physical fields.

In this study, hierarchically bionic porous phase change materials were prepared by imitating natural systems combining superior thermal conductivity and phase change characters. The prepared hierarchically bionic porous phase change materials were considered, then the thermo-physical properties and optical properties were discovered. Therefore, a magnetically-accelerated solar-thermal energy storage method was suggested. Solid-liquid phase transition research with hierarchically bionic porous phase change materials was conducted, comparing to pure paraffin wax. In addition, the efficiency and storage capacity of various heat transfer performances were determined for the evaluation of the influence of the hierarchically porous structure and magnetism on phase change performances. Finally, the heat transfer process of photo-thermal energy conversion and storage in hierarchically porous materials under an external physical field was verified by simulation.

2. Experimental research

2.1. Material preparation

To create an ultrapure water system in the lab, deionized (DI) water purification was performed, along with other experiments (Arium-mini plus, Sartorius, Germany). Firstly, the iron (III) chloride hexahydrate was thoroughly mixed for 10 minutes in the DI. Next, sodium citrate was added and mixed in the suspension and urea by ultrasonic agitation. Later, the suspension and polyacrylamide were mixed together completely for 15 min. A100 mL flask set at 160°C immersed in a water bath for 8h was used to transfer the final solution. Subsequently, ethanol was used to wash the black precipitates magnetic Fe_3O_4 composites through magnetic attraction prior to oven drying at 50 °C for 12 h. The MF nanoparticles were gradually mixed into the 40 mmol titanium (IV) tetrafluoride solution which was then stirred for 10 minutes. After this, the solution was moved into and placed in a Teflon-sealed autoclave and maintained at a temperature of 180 °C for 48 h. Finally, the poriferous magnetic TiO_2 (MT) was stirred vigorously in liquid paraffin wax (PW) within 5 wt.% to prepare the poriferous paraffin@magnetic TiO_2 (PMT). The MF was stirred vigorously in liquid paraffin wax within 5 wt.% to prepare the poriferous paraffin@magnetic Fe_3O_4 (PMF). All above drugs were purchased from

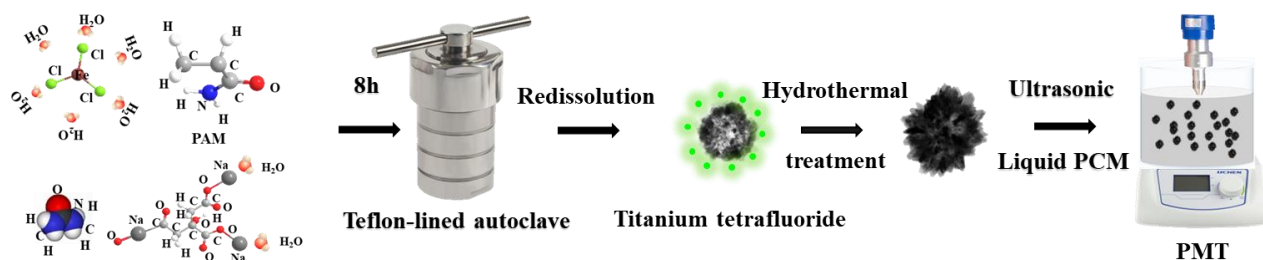Aladdin Reagent (Shanghai, China) within the analytical reagent grade and were used as received.

Figure 1. Preparation of the paraffin@magnetic Fe_3O_4 (PMF) and paraffin@magnetic TiO_2 (PMT)

2.2. Characterisation

To further confirm the particles, the MF and MT nanomaterials were characterised by the scanning of microscopy regarding electrons (SEM, Zeiss Supra 55, Germany) along with transmission electron microscopy (TEM, 2010-JEM, Japan). An X-ray diffraction (XRD) pattern was gained using an X-ray diffractometer (AXS-Bruker GmbH, Germany, D8-Advance). Brunauer-Emmett-Teller (BET) was used in order to gain analysis of the particle size and surface area of the pores (Quantachrome Autosorb-1C-VP, US). Magnetism of nanoparticles was achieved by using a vibrating sample magnetometer (SQUID VSM-MPMS, Design Quantum, USA). The PCM's thermo-physical properties, thermal conductivities, and particular heat volume and optical properties were determined using an ultraviolet-visible-near-infrared spectrophotometer (5000-CARY, Technology of Agilent, USA), a laser thermal diffusivity instrument (LFA 457, Netzsch, Germany), and a differential scanning calorimetry system (F1-204, Netzsch, Germany).

2.3. Experimental setup

The solar-thermal energy storage method is inspired by imitating natural systems in the ocean. Diatoms can track light sources through the holes in pores in order to capture solar energy by reflecting less sunlight. The silk network structure of diatoms not only prevents incident light from escaping and enhances their absorption, but it also enhances their adsorption and storage capacities within flexible and stable structures (Figure 2a). Based on this, bionic phase change composites within a hierarchical porous structure were prepared and a magnetically-accelerated method was developed for energy storage and solar-thermal conversion. The experimental setup is shown in Figure 2b: the light source used in the experiment was a sunlight simulator (CEL HXF300, Ceaulight, China) with a constant solar intensity (1000 W/m^2), a magnetism generator (ELE-P80, Elecall, China) whose intensities were measured by a magnetometer (M943, Honor Top of Magnetic Technology, China); Test chamber (an

acrylic beaker), thermocouples, a data collector, and a computer form a data collection system. The chamber had a 3.0 cm height and 4.0 cm diameter. In addition, temperature readings were obtained from the five thermocouples inserted in the middle of the sample to record temperature changes and noted by a data collection unit (CA34972, Technology of Agilent).
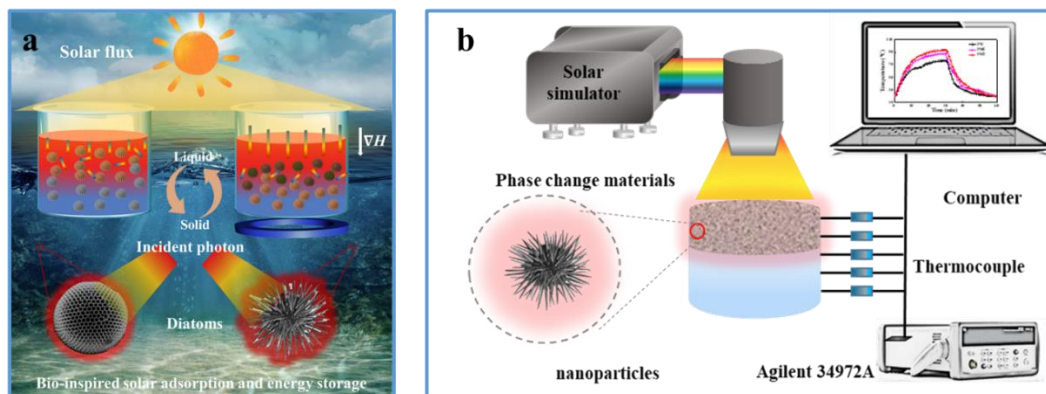

Figure 2. (a) The schematic diagram of magnetically-accelerated method for solar absorption based on bio-inspired hierarchical porous phase change composites; (b) schematic of the experimental facility for energy storage through solar-thermal conversion of magnetic phase change composites

3. Results and discussion

3.1. Characterisation of nanoparticles and composites

SEM images depicted the shape of the prepared MF within uniform morphologies and well-dispersed properties (Figure 3a). From Figure 3b and Figure 3c, it can be seen that the darkness of MF and MT are heterogeneously distributed, which could indicate that the nanoparticles have porous structure. For further clarification, the specific surface area of MT and MF was observed in the pore distributions and N_2 adsorption-desorption isotherms (Figure 3d). The BET surface area was measured to be as high as 184.6 m^2 g^{-1} (MT), compared to the 146.2 m^2 g^{-1} MF nanoparticles, which were the result of their hierarchical pores within the nano-structure, visible in the desorption-adsorption isotherms and the distributions of pores. The diffraction peaks at 2θ=21.6° and 23.5° were due to the (110) and (200) reflection of paraffin wax (Figure 3e). The diffraction peaks detected at 2θ angles of 24.9°, 37.6°, 48.1°, 54.8° and 62.6°, corresponded to the (110), (112), (101), (004) and (200) reflections of TiO_2 (PDF No. 65-1119). Other diffraction peaks well matched the (220), (311), (400), (422), (511) and (440) likenesses of the magnetism phase (JCPDS No. 89-0691) [7]. The magnetisation of the magnetic PMT (4.8 emu/g) was transformed into MT (64.7 emu/g) on the basis of the measured weight percentage (Figure 3f).
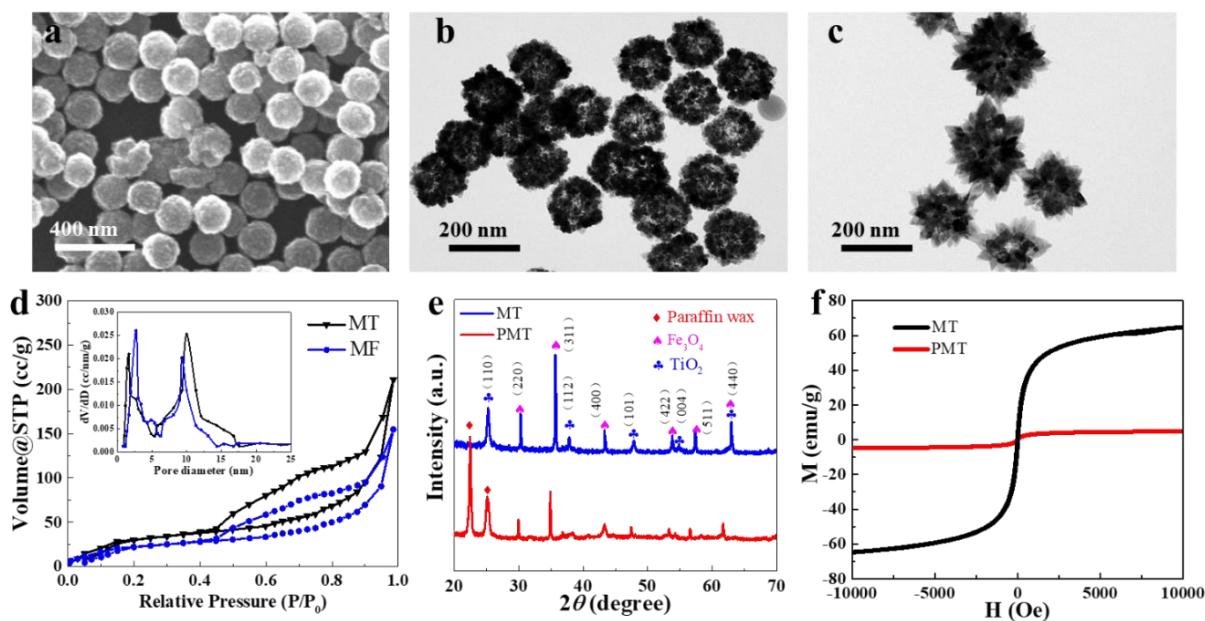
Figure 3. Structural characterisation of nanoparticles and composites: (a) scanning electron microscopy (SEM) images of MF; TEM images of the (b) MF and (c) MT; (d) Pore size distributions and N_2 adsorption-desorption isotherms of the MF and MT; (e) X-ray diffraction patterns and (f) hysteresis loops of the MT and PMT

Figure 4a shows the specific heat capacity in the phase change regions for different phase change composites with the temperature of 10~110°C, which was used to calculate the energy storage capacity. The value of the specific heat of solid (2.56 J/(°C·g)) is less than that of liquid (2.97 J/(°C·g)) of the PW, which are similar to the standard specific heat of paraffin wax (2.60 J/(°C·g) and 2.89 J/(°C·g)). It can be seen that the specific heat of the phase change composites had no obvious change during the melting and freezing process when adding nanoparticles. This indicates that magnetic nanoparticles within small mass concentration in phase change materials have a weak influence on heat storage capacity. Figure 4b displays the thermal conductivities of the PW, PMF and PMT over a temperature range of 30~90°C. The outcome showed a vibrant change in thermal conductivity when the nanoparticles were inserted into both liquid and solid forms of paraffin wax. PMT had a higher thermal conductivity, compared to PMF. PW had greater transmission in the instance of the liquid state in the noticeable range of light (Figure 4c), but the transmission of PMF and PMT was close to zero, due to the robust photo-absorption capacity of the nanostructure. It also can be seen that PMT has superior optical absorption performance. The transmission of different weight percentages of PMT were further characterized (Figure 4d). It can be seen that the transmittance of PMT was decreased with the increase of mass concentration at first, and it has no change when further increasing the mass concentration of

nanoparticles, which is in order to determine the best mass concentration (5 wt. %) to conduct the solar-thermal conversion and phase change experiments [2,5].
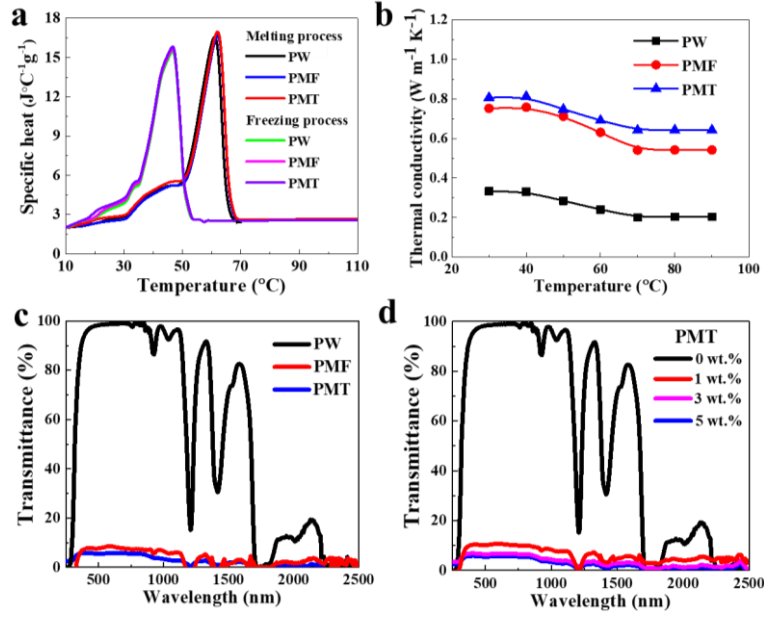

Figure 4. (a) Specific heat capacity over the temperature range of 10~110°C, (b) conductivity over the temperature range of 30~90°C, and (c) transmittance of the phase change composites (PW, PMF, and PMT) at 80°C. (d) transmittance of different weight percentages of PMT at 80°C

3.2. Solar-thermal conversion and phase change characteristics

In order to further examine the solar-thermal conversion and heat transfer performance of phase change composites, both were determined based on the temperature variation and measured particular heat of the PCMs [2,21]:

$$Q_e = m \int c_p(T) dT \tag{1}$$

$$\eta_s = \frac{Q_e}{q_{solar} S t} \tag{2}$$

$$\eta_r = \frac{Q_e}{Q_{max}} \tag{3}$$

where Q_e is energy conversion capacity (storage or discharge) at time t, S is the direct solar area, q_{solar} is the solar radiation power, m is the mass, c_p is the specific heat capacity, T is the temperature of the PCMs, and η_s and η_r are the heat storage/discharge efficiency. Optimal heat transfer and solar absorption are two requirements for achieving high energy conversion efficiency during the solar-thermal conversion process. Therefore, based on the magnetism and absorbance of the bionic hierarchical porous materials, the effect of magnetic nanoparticles on phase change characteristics was

investigated, and the mechanism of magnetically enhanced solar-thermal conversion was researched.

3.2.1 Influence of the magnetic nanoparticles on phase change characteristics

The phase change composites melt robustly via straight solar radiation and the localized heating area shifts downwards by heat conduction. The experiments of phase change characteristics under solar illumination with PMF and PMT composites were conducted and compared with PW. Figure 5a shows the change in temperature at the time of changing processes. Compared to PW and PMF, the temperature of PMT increases rapidly during the charging process and has a higher steady temperature (94.2°C) due to its superior solar absorption ability and high thermal conductivity. For the release energy process, the temperature dropped rapidly initially and gradually achieved a stable state as a result of heat release and dissipation. To clarify the heating and cooling processes of phase change materials through solar irradiation, their rates of cooling and heating regarding time are shown in Figure 5b and Figure 5c. The initial peak of heating rate could be attributed to the specific heat capacity change in the process of the melting of the composite. The improved solar absorption ability of the liquid phase change materials, in addition to the latent heat effect disappearance, could be the source of the second peak. The heat storage/discharge capacity (Figure 5d) showed that the solar-thermal storage capacity of PMF and PMT had significant enhancements and contained at 353.2 J/g and 377.6 J/g, which respectively increased by 14.8% and 22.7%, compared to that of the PW (307.7 J/g). The heat storage/discharge efficiency was determined by Equation (2) and Equation (3) on the basis of the heat storage/discharge capacity (Figure 5e and Figure 5f). The storage efficiency of the phase change materials improved initially and then reduced to a steady state, and the maximum storage efficiency of the PMF and PMT increased by 67.6% and 102.7%, compared to that of the PW. The discharge efficiency of the phase change materials was increased to a steady state which is consistent with the maximum storage efficiency. During the heat storage/discharge process, heat loss is minimal when the temperature is low, and many absorbed solar energies are utilised in phase change enthalpy which improves the efficiency of storage. At the time of the solid phase changing to the liquid phase, the increased temperature results in a greater loss of heat, and the volumetric efficiency decreases in relation to the improvement of illumination with time. In contrast, when the liquid phase changes to the solid phase, the discharge efficiency increases with time. In summary, the combination of magnetic nanoparticles enhances thermal conductivity, accelerates capacity efficiency, upsurges solar energy absorption, and increases storage capacity.
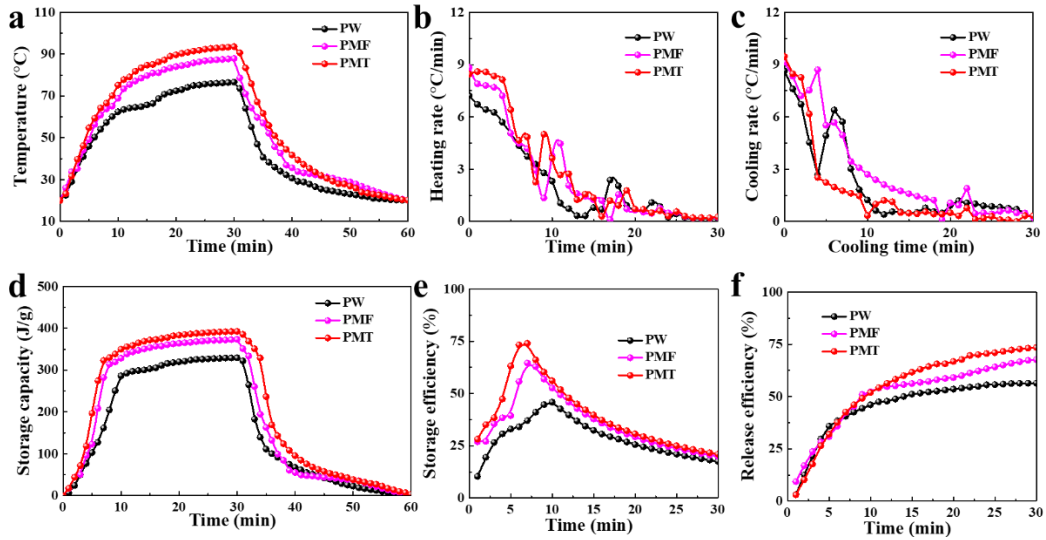
Figure 5. Heating and cooling processes of PW, PMF and PMT. (a) temperature changes, (b) heating rate and (c) cooling rate as a function of heating time; Release characteristics and thermal storage of PW, PMF and PMT. (d) thermal storage capacity, (e) thermal storage efficiency and (f) thermal release efficiency as a function of heating time

3.2.2 Enhanced magnetically solar-thermal conversion process

Under simulated solar irradiation, when a solid PMT converts the liquid phase and also following a reduction in viscosity, the particles within magnetism become firmly combined to the paraffin. At the same time, the solar-absorbed nanoparticles are formed under magnetically volumetric force towards the solid-liquid phase interface. Therefore, the thermal-solar conversion takes place during the interface phase, mainly because of upper liquid paraffin layer, where due to no presence of nanoparticles, the transmission is high. After the experiment, the PMT's steady temperature improved from 94.2°C to 103.9°C (Figure 6a) when applying the magnetic field. Initially, the change of phase was mainly due to thermal diffusion, while the magnetic nanoparticles changed into the new liquid-solid phase interphase as more PMT was shifted into liquid phase with the help of magnetic volumetric force. The higher peak of heating rate could be attributed to magnetic nanoparticle movement in the composite melting process, which is shown in Figure 6b. The magnetism nanoparticles displayed a larger volumetrically magnetic force and shifted more quickly at the time of magnetism. Therefore, a large amount of concentrations of nanoparticles gathered in the interface phase and the upper PMT possess high transmission, which promotes superior efficiency of solar-thermal conversion process, causing phase transition enthalpy. As shown in Figure 6c, the magnetically controlled heat shift method reflected the improved storage capability, approximately 20.3% greater than that without magnetic field. The thermal-solar storage efficiencies exhibited rapid charging rate improvement in the initial

stage with magnetic field strength and the highest storage efficiency was approximately 27.1% greater than that without magnetic field, as shown in Figure 6d. In order to further explain the mechanism of magnetically enhanced solar-thermal conversion, a two-dimensional mathematical model was created using commercial software assuming Newtonian, laminar and incompressible flow. The size and boundary conditions used for the simulation were consistent with the experiment. Material properties were applied to simulation in the form of piecewise functions of experimental values. From the simulation results and using the finite element method (Figure 6e), the PMT's changes in temperature exhibited similar features to the research outcomes. By applying the magnetic field, the PMT temperature increased rapidly. The velocity distribution and magnetic field of PMT liquid showed that the circulation was initiated by using volumetric magnetism power. In addition, the normal volumetric magnetic force formed at the phase interface also increased the melting of paraffin. Table 1 concluded the comparison of phase change performance parameters of PW, PMF, and PMT without and with the magnetic fields. The numerical average temperature of the PMT was 372.6 K, which is similar to the outcome of the experiment (377.1 K). Comparison of experimental results with theoretical results was showed in Figure 6f with error bar. It can be seen that the numerical average temperature of the PMT was similar to the outcome of the experiment, and the errors are 1.7% without magnetic field and 1.2% with magnetic field.
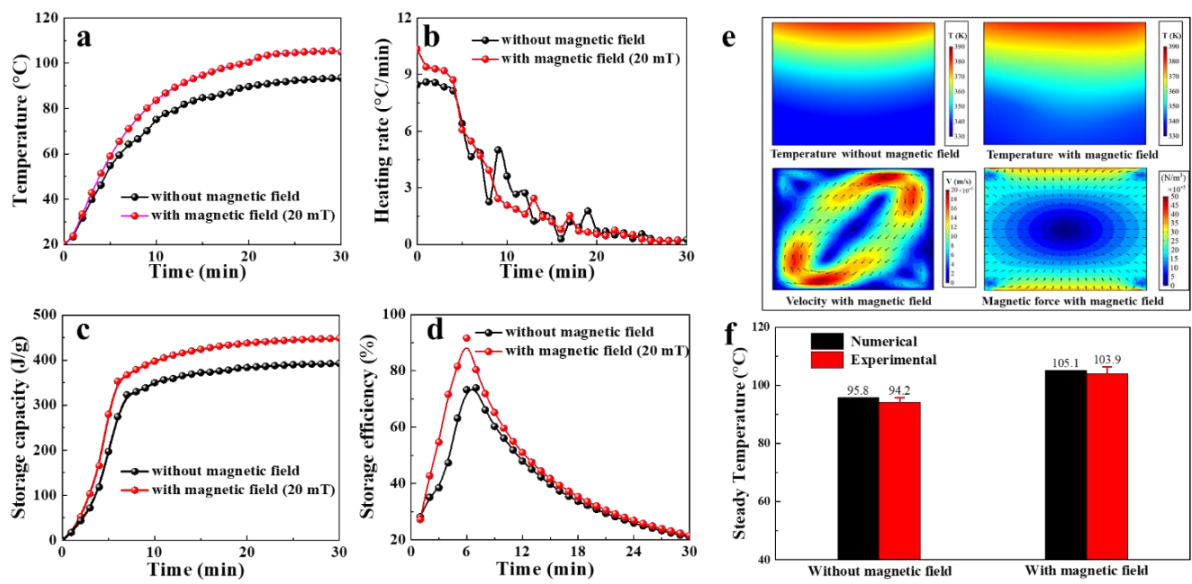

Figure 6. The influence of the magnetic field on photo-thermal conversion. (a) temperature changes, (b) heating rate and (c) thermal storage capacity; (d) thermal storage efficiency as a function of heating time (e) magnetically enhanced mechanism for heat transfer: the distribution of temperature, velocity and magnetic force; (f) experimental and numerical steady temperature with and without magnetic field during the phase change process

Table 1 Phase change performance of PW, PMF, and PMT without and with the magnetic fields

Phase change performance		PW	PMF	PMT
Steady temperature (ºC)	Without magnetic field	75.7	88.6	94.2
	With magnetic field (20 mT)	-	97.5	103.9
Storage capacity (J/g)	Without magnetic field	307.4	353.3	377.8
	With magnetic field (20 mT)	-	416.7	448.4

4. Conclusion

In the current study, phase change materials with hierarchical bionic porous were formed with the help of a two-step method with paraffin wax and porous magnetic nanoparticles. The morphology, specific surface area and magnetism of different particles were characterised, and the thermo-physical characteristics of hierarchically bionic porous phase change materials were further evaluated. A magnetically-accelerated solar-thermal energy storage method effectively was established by imitating natural systems, combining the nanomaterial characteristics of magnetism and superior thermal conductivity. Energy storage and release experiments were conducted in order to evaluate the phase change features of different phase change composites compared to pure paraffin. The storage efficiency of the phase change materials improved during the initial stage and then reduced to a stable state, and the maximum storage efficiency of the PMT increased by 102.7%, compared to that of the PW.

Energy storage experiments and solar-thermal conversion reflected that the efficiency of phase change of hierarchically bionic porous materials can be further improved by magnetism. At the time of solar irradiation process, the photo-absorbed nanomaterials are concerned with moving to the interface of liquid-solid phase under the magnetic field. Therefore, the storage efficiencies of the solar thermal possess robust charging rate combined with magnetism power improvement at the starting point, and the highest storage efficiency was recorded at approximately 27.1% more than that without the magnetic field. A large number of photons were transformed into thermal energy with the help of solar-thermal conversion, and provided phase transition enthalpy at the time of the phase interface. At the same time, the heat transfer process of energy storage and solar-thermal conversion in hierarchically porous materials under the external physical fields was explained by simulation.

Acknowledgements

References

[1] Xiao X, Jia H, Wen D, Zhao X. Thermal performance analysis of a solar energy storage unit encapsulated with HITEC salt/copper foam/nanoparticles composite. Energy, 2020, 192: 116593.

[2] Chen M, He Y, Ye Q, Zhang Z, Hu Y. Solar thermal conversion and thermal energy storage of CuO/Paraffin phase change composites. International Journal of Heat and Mass Transfer, 2018, 130: 1133-1140.

[3] Cheng Z, He Y, Cui F. A new modelling method and unified code with MCRT for concentrating solar collectors and its applications. Applied Energy, 2013, 101: 686-698.

[4] Karami M, Akhavan-Behabadi M, Dehkordi M, Delfani S. Thermo-optical properties of copper oxide nanofluids for direct absorption of solar radiation. Solar Energy Materials and Solar Cells, 2016, 144: 136-142.

[5] Wang, X, He Y, Liu X, Shi L, and Zhu J. Investigation of photothermal heating enabled by plasmonic nanofluids for direct solar steam generation. Solar Energy, 2017, 157: 35-46.

[6] Zeng J, Xuan Y. Enhanced solar thermal conversion and thermal conduction of MWCNT-SiO$_2$/Ag binary nanofluids. Applied Energy, 2018, 212: 809-819.

[7] Mahian O, Kianifar A, Heris S, Wen D, Sahin A, Wongwises S. Nanofluids effects on the evaporation rate in a solar still equipped with a heat exchanger. Nano Energy, 2017, 36:134-155.

[8] Shi L, Wang X, Hu Y, He Y. Recyclable solar-thermal conversion and purification systems via Fe$_3$O$_4$@TiO$_2$ nanoparticles. Solar Energy, 2020, 196: 505-512.

[9] Liu J, Ye Z, Zhang L, Fang X, Zhang Z. A combined numerical and experimental study on graphene/ionic liquid nanofluid based direct absorption solar collector. Solar Energy Materials and Solar Cells, 2015, 136: 177-186.

[10] Sun J, Song L, Fan Y, Tian L, Luan S, Niu S, Zhao, J. Synergistic photodynamic and photothermal antibacterial nanocomposite membrane triggered by single NIR light source. ACS applied materials & interfaces, 2019, 11(30): 26581-26589.

[11] Wang Y, Wang L, Xie N, Lin X, Chen H. Experimental study on the melting and solidification behavior of erythritol in a vertical shell-and-tube latent heat thermal storage unit. International Journal of Heat and Mass Transfer, 2016 99: 770-781.

[12] Yu Y, Tao Y, He Y. Molecular dynamics simulation of thermophysical properties of NaCl-SiO$_2$ based molten

salt composite phase change materials. Applied Thermal Engineering, 2019: 114628.

[13] Pereira J, Eames P. Thermal energy storage for low and medium temperature applications using phase change materials-A review. Applied Energy, 2016, 177: 227-238.

[14] Feng D, Feng Y, Qiu L, et al. Review on nanoporous composite phase change materials: Fabrication, characterization, enhancement and molecular simulation. Renewable and Sustainable Energy Reviews, 2019, 109: 578-605.

[15] Li D, Cheng X, Li Y, Zou H, Yu G, Li G, Huang Y. Effect of MOF derived hierarchical Co_3O_4/expanded graphite on thermal performance of stearic acid phase change material. Solar Energy, 2018, 171: 142-149.

[16] Li Y, Yu S, Chen P, Rojas R, Hajian A, Berglund L. Cellulose nanofibers enable paraffin encapsulation and the formation of stable thermal regulation nanocomposites. Nano Energy, 2017 34: 541-548.

[17] Deng Z, Liu X, Zhang C, Huang Y, Chen Y. Melting behaviors of PCM in porous metal foam characterized by fractal geometry. International Journal of Heat and Mass Transfer, 2017, 113: 1031-1042.

[18] Tasnim, SH, Hossain R, Mahmud S, Dutta A. Convection effect on the melting process of nano-PCM inside porous enclosure. International Journal of Heat and Mass Transfer, 2015, 85: 206-220.

[19] Zhang Q, Wang H, Ling Z, Fang X, Zhang Z. RT100/expand graphite composite phase change material with excellent structure stability, solar-thermal performance and good thermal reliability. Solar Energy Materials and Solar Cells, 2015, 140: 158-166.

[20] Wang W, Tang B, Ju B, Gao Z, Xiu J, Zhang S. Fe_3O_4-functionalized graphene nanosheet embedded phase change material composites: efficient magnetic-and sunlight-driven energy conversion and storage. Journal of Materials Chemistry A, 2017, 5(3): 958-968.

[21] Sheikholeslami M. Solidification of NEPCM under the effect of magnetic field in a porous thermal energy storage enclosure using CuO nanoparticles. Journal of Molecular Liquids, 2018, 263: 303-315.

[22] Wang L, Zhang J, Wang Y, Lin X, Xie N, Chen H. Experimental study on natural convective heat transfer of tube immersed in microencapsulated phase change material suspensions. Applied Thermal Engineering, 2016, 99: 583-590.

[23] Liu J, Chen L, Fang X, Zhang Z. Preparation of graphite nanoparticles-modified phase change microcapsules and their dispersed slurry for direct absorption solar collectors. Solar Energy Materials and Solar Cells, 2017, 159: 159-166.

[24] Yu Q, Lu Y, Zhang C, Wu Y, Sunden B. Research on thermal properties of novel silica nanoparticle/binary nitrate/expanded graphite composite heat storage blocks. Solar Energy Materials and Solar Cells, 2019, 201:

110055.

[25] Wu W, Wu W, Wang S. Form-stable and thermally induced flexible composite phase change material for thermal energy storage and thermal management applications. Applied Energy, 2019, 236: 10-21.

[26] Lv P, Liu C, Rao Z. Review on clay mineral-based form-stable phase change materials: preparation, characterization and applications. Renewable & Sustainable Energy Reviews, 2017, 68: 707-726.

[27] Khodadadi J M, Hosseinizadeh S F. Nanoparticle-enhanced phase change materials (NEPCM) with great potential for improved thermal energy storage. International Communications in Heat and Mass Transfer, 2007, 34(5): 534-543.

[28] Bahraseman H, Languri E. East J. Fast charging of thermal energy storage systems enabled by phase change materials mixed with expanded graphite. International Journal of Heat and Mass Transfer, 2017, 109: 1052-1058.

[29] Feng Y, Li H, Li L, Bu L, Wang T. Numerical investigation on the melting of nanoparticle-enhanced phase change materials (NEPCM) in a bottom-heated rectangular cavity using lattice Boltzmann method. International Journal of Heat and Mass Transfer, 2015, 81: 415-425.

[30] Xu B, Zhou J, Ni Z, Zhang C, Lu C. Synthesis of novel microencapsulated phase change materials with copper and copper oxide for solar energy storage and solar-thermal conversion. Solar Energy Materials and Solar Cells, 2018, 179, 87-94.

[31] Sarı A, Biçer A, Hekimoğlu G. Effects of carbon nanotubes additive on thermal conductivity and thermal energy storage properties of a novel composite phase change material. Journal of Composite Materials, 2019, 53(21): 2967-2980.

[32] Fadl M, Eames P C. A comparative study of the effect of varying wall heat flux on melting characteristics of phase change material RT44HC in rectangular test cells. International Journal of Heat and Mass Transfer, 2019, 141: 731-747.

[33] Languri EM, Rokni HB, Alvarado J, Takabi B, Kong M. Heat transfer analysis of microencapsulated phase change material slurry flow in heated helical coils: A numerical and analytical study. International Journal of Heat and Mass Transfer, 2018, 118: 872-878.

[34] Viskanta R. Phase-change heat transfer. Solar Heat Storage. CRC Press, 2018: 153-222.

[35] Liang W, Wang L, Zhu H, Pan Y, Zhu Z, Sun H, Li A. Enhanced thermal conductivity of phase change material nanocomposites based on MnO2 nanowires and nanotubes for energy storage. Solar Energy Materials and Solar Cells, 2018, 180: 158-167.

[36] Águila B, Vasco D, Galvez P, Zapata P. Effect of temperature and CuO-nanoparticle concentration on the thermal

conductivity and viscosity of an organic phase-change material. International Journal of Heat and Mass Transfer, 2018, 120: 1009-1019.

[37] Oya T, Nomura T, Tsubota M, Okinaka N, Akiyama T. Thermal conductivity enhancement of erythritol as PCM by using graphite and nickel particles. Applied Thermal Engineering, 2013, 61(2): 825-828.

[38] Nourani M, Hamdami N, Keramat J, Moheb A, Shahedi M. Thermal behavior of paraffin-nano-Al_2O_3 stabilized by sodium stearoyl lactylate as a stable phase change material with high thermal conductivity. Renewable Energy, 2016, 88: 474-482.

[39] Mei S, Qi C, Luo T, Zhai X, Yan Y. Effects of magnetic field on thermo-hydraulic performance of Fe_3O_4-water nanofluids in a corrugated tube. International Journal of Heat and Mass Transfer, 2019, 128: 24-45.

[40] Shi L, Hu Y, He Y. Magneto-responsive thermal switch for remote-controlled locomotion and heat transfer based on magnetic nanofluid. Nano Energy, 2020, 71: 104582.

[41] Shi L, Hu Y, He Y. Magnetocontrollable convective heat transfer of nanofluid through a straight tube. Applied Thermal Engineering, 2019, 162: 114220.